ZIBELINE INTERNATIONAL PUBLISHING

Malaysian Journal of Geosciences (MJG)

DOI: http://doi.org/10.26480/mjg.01.2020.07.12

ISSN: 2521-0920 (Print)
ISSN: 2521-0602 (Online)
CODEN: MJGAAN

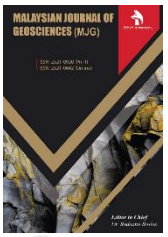

RESEARCH ARTICLE

CLASSIFICATION OF HIGH-RESOLUTION SATELLITE IMAGES USING FUZZY LOGICS INTO DECISION TREE

Ehsan Momeni[a], Mahmoud Reza Sahebi[b], Ali Mohammadzadeh[b]

[a] Department of Earth Sciences, The University of Memphis, 445 State, Memphis, TN 38111, USA
[b] Faculty of Geodesy and Geomatics Engineering, K. N. Toosi University of Technology, No. 1346, ValiAsr Street, Mirdamad cross, Tehran, Iran
Corresponding Author Email:* **hsn.momeni@gmail.com

ARTICLE DETAILS

Article History:

Received 05 December 2019
Accepted 12 January 2020
Available online 05 February 2020

ABSTRACT

In this paper, DTFL an image classifier based on Decision Tree and Fuzzy Logics is proposed. At the beginning of classification using DTFL, each pixel is located at the highest level of a decision tree where it belongs to the combination of all classes. DTFL transfers a pixel to a lower level of the decision tree where the pixel belongs to a combination of fewer classes. Decision-making about transfers is based on fuzzy logic with seven different membership functions including triangular-shaped, trapezoidal-shaped, π-shaped, bell-shaped, Gaussian, differential S-shaped and multiplicative S-shaped. Eventually, pixels will reach the lowest level of the decision tree where it belongs to only one class. For accuracy assessment, DTFL was used to classify a GeoEye-1 image. The overall accuracy of 96.14% and a kappa coefficient of 96.06% were reached by DTFL. In comparison, the overall accuracy of 89.91% and a kappa coefficient of 89.77% were reached by a Maximum Likelihood Classifier, MLC. In the case of applying a threshold in MLC to reach the same accuracy as DTFL, 8.73% of pixels take the non-classified label while using DTFL all the pixels get a proper label. The results indicate that the proposed classifier extracts more information from images.

KEYWORDS

supervised classification, GeoEye-1, fuzzy membership function, decision tree, Iran.

1. INTRODUCTION

During the last decades, a wide range of pattern recognition techniques has been invented to extract information from remotely sensed data such as satellite images. Meanwhile, the flexibility and performance of image classifiers make them one of the main recognition techniques for extracting information from satellite images. Image classification is defined as a decision-making process in which a label of a class (or more classes) is assigned to each pixel of an image with the maximum confidence of assignment (Gomez et al., 2016; Momeni, 2011). Traditional image classification methods carry out a hard classification output based on the fundamental law of "one pixel-one class". The fundamental law clears that a pixel is either a full member of a class or not. Consequently, traditional image classification methods are not considered as the best method for classifying mixed or imprecise pixels in an image (Momeni, 2011). On the other hand, advanced image classification methods, such as genetic algorithms and expert systems, have many issues with image classification, such as no general standards for defining the architecture, training requirements and time-consuming training (Gomez et al., 2016; Ghosh et al., 2014).

In recent decades, fuzzy logic has been implemented in various fields of study such as control systems, image processing and classification of remotely sensed data (Momeni, 2011; Zimmermann, 2011). A fuzzy classifier estimates the contribution of each class in each pixel. In other words, a fuzzy classifier assumes that each pixel in the image is a decomposable unit and, accordingly, works on a new fundamental law of "one pixel-several class" to extract more information about pixels (Momeni, 2011; Ghosh et al., 2010; Dutta, 2009). A group researchers, provided a survey on different image classification methods and concluded fuzzy logic as one of the most reliable image classification methods (Akgun et al., 2004; Weng and Lu, 2007). In addition, some other scholars have investigated applications of fuzzy image classification and claimed that fuzzy classifiers are among the most powerful tools for the classification of satellite images (Bai et al., 2014; Xu et al., 2019; Joseph and Chockalingam, 2017). Pixel-based classification is still among the most practical classification approaches due to simplicity, low computational cost and high reliability (Gonzalez et al., 2016). However, pixel-based classification is not accurate to classify mixed pixels with overlapped spectral characteristics. Even though applying thresholds can increase the accuracy and reliability in the labeling of pixels, but thresholds omit some of the mixed pixels from the classification process. In that case, omitted pixels get a non-classified label (Momeni, 2011; Joseph and Chockalingam, 2017).

This paper is aimed to introduce a novel satellite images classifier, called DTFL, based on a Decision-Tree and Fuzzy Logic. DTFL is able to classify all the pixels in an image and avoids non-classified labeling. It also takes the advantages of fuzzy concepts to increases the accuracy of classification in comparison with traditional classifiers such as Maximum Likelihood (ML). In order to assess the performance of the proposed classifier, DTFL was used in the classification of a high-resolution GeoEye-1 satellite image of the Azadi Complex, Iran, and the results were compared with the results of image classification using the ML classifier. Using an advanced image

Quick Response Code	Access this article online	
	Website: www.myjgeosc.com	DOI: 10.26480/mjg.01.2020.07.12

Cite the Article: Ehsan Momeni, Mahmoud Reza Sahebi, Ali Mohammadzadeh (2020). Classification Of High-Resolution Satellite Images Using Fuzzy Logics Into Decision Tree. *Malaysian Journal of Geosciences, 4(1): 07-12.*

classifier such as DTFL helps the city and regional planners to understand their surroundings more precisely to offer a more reliable plan for the future of the region. In particular, regional farm managers can estimate the amount of different agricultural products more precisely and will make key strategic plans based on more accurate knowledge. The rest of this paper is organized as the following: Section Two describes the proposed DTFL classifier. The principal of the decision tree approach and different fuzzy membership functions, as well as different reasoning rules, are discussed in the same section. A brief description of datasets and results of using DTFL for classification is discussed in Section Three. Section Four is dedicated to discussions and lastly, the concluding remarks are given in Section Five.

2. METHODOLOGY

DTFL is a sub-pixel supervised classification method based on the tree method and fuzzy logic. At the beginning of the image classification using DTFL, each pixel is located at the highest level of a decision tree. Each level represents the number of confusions in the classification. Each pixel belongs to the combination of all the initial classes at the highest level of the decision tree. DTFL classifies each pixel in a smaller combination of classes by defining a hypothesis. The hypothesis is based on the transfer of each pixel from a higher level to a lower level and needs validation. Decision making about the transfer of each pixel to a lower level is based on fuzzy logic. Using an iterative process, each pixel is transferred from the higher level to the lower one (Figure 1). The iterative process continues until either of the two following conditions is satisfied:

A) A state having a single class (called a leaf) is reached

B) No new state is reached after the iteration

In the first case, the pixel is classified as a pure pixel and get a single label while in the latter case, the pixel is classified as a mixed pixel and get a label according to its level on the tree (avoids non-classified label).

2.1 Decision Tree

Decision Tree (DT) classification is a hierarchical process where at each level, a test is applied to one or more attribute values and makes one or more outcomes. The outcome(s) may be either a leaf resembling a class (or more classes) or a decision node (or more decision nodes) describing a further test on the attribute values which creates a branch or sub-tree of the tree (Al-Obeidat et al., 2015). The classification process is completed by passing the pixel down the tree until either a leaf is reached or no new state is reached after the iteration. In the latter case, the pixel is classified as a mixed pixel and get a proper label according to its level. The structure of a decision tree classifier is shown in Figure 1 (Momeni, 2011).

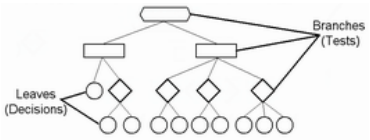

Figure 1: Structure of a decision tree classifier (Momeni, 2011)

2.1.1 Schematic presentation of a decision tree

Consider a multispectral image of an area whose pixels have to be classified. Let's assume CL as the set of all *k* possible classes. Each pixel in the image has to be classified into one or more (for mixture pixels) of the *k* possible classes in CL. Figure 2 shows the outline of interpreting a pixel in a four-classes problem (*k*=4) where CL= {C_1, C_2, C_3, C_4}.

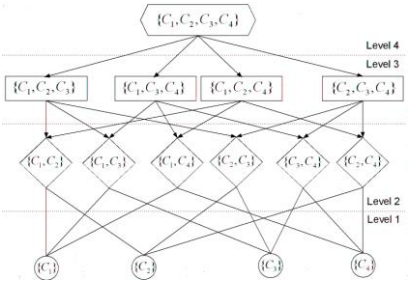

Figure 2: Outline of interpreting a pixel in a decision tree classification with four initial classes (Momeni, 2011)

Each node in Fig represents a state of uncertainty for the pixel during the classification. For instance, the node {C_1, C_2} indicates the state: "The pixel may belong unconditionally to the C_1 or unconditionally to the C_2 or to a combination of C_1 and C_2". The connector lines in Figure 2 represent hypotheses through which state transfers can occur. For instance, the connector line between {C_1, C_2, C_3} and {C_1,C_2} indicates the hypothesis that: "The pixel belongs to one or more classes in the set of {C_1, C_2} with the assumption that it belongs to one or more of classes in the set of {C_1, C_2, C_3}". The inference mechanism chooses appropriate hypotheses to test. Each hypothesis is either true or false. According to the results of those tests, the inference mechanism infers the new state of the pixel.

2.1.2 Inference mechanism

The interpretation of a pixel is an iterative process of inference. Each iteration includes three steps:

Step1: selecting appropriate hypothesis for the test;
Step2: testing the validity of the selected hypothesis;
Step3: analyzing the passed hypothesis in order to infer the next state.

The iterative process continues until either of the following conditions is satisfied:

A) A state with a single class (a leaf) is reached (e.g., states {C_1} or {C_2}). In such cases, a solid decision is reached and the pixel gets a single label of the class; or

B) No new state is reached after iteration. In such cases, a solid decision could not be reached either due to lack of knowledge or due to the case of a mixed pixel (e.g., pixel covering more than one land cover classes). In such cases, the pixel is considered as a mixed pixel and get a proper label of classes.

The decision in the latter case assigns a set of possible classes to the pixel and avoids the non-classified label. For example, assigning {C_1, C_2} to a pixel means the pixel is a mixture of class {C_1} and {C_2} and other classes (such as {C_3} or {C_4}) have no contributions in the pixel. In comparison, traditional classifiers such as MLC, omit mixed pixels and simply assign a non-classified label to them.

2.1.3 Selecting appropriate hypotheses

As Figure 2 shows, classification schema is separated into different levels based on the number of classes each level contains. In other words, the level of a state indicates the degree of uncertainty. For instance, four possible states are available at the level-3, where each of them is a unique combination of three land cover classes. Consequently, at any given state such as S, the set of possible hypotheses is in the form of $S \rightarrow D$, where $D \subset S$. The sublevel of a hypothesis $S \rightarrow D$ is defined as *d* where *d* is the level of *D* (e.g., the number of classes in *D*). The process of inferring always starts at the maximum uncertainty and the first sublevel. The process then continues iteratively. At the end of each iteration, the new states and sublevels are deduced for the next iteration.

2.1.4 Testing chosen hypotheses

For testing the chosen hypotheses, appropriate rules must be selected and their validity should be verified. The basic representation of rules is as the following (Equ. 1):

BASE RULE: IF [CL_1, ..., CL_n] THEN hypotheses H_0 is true (Equ. 1)

Where CL_i is logical constraints on one or more attributes of pixels.
In a real classification problem usually more than one rule is defined. In that case, if R_1,..., R_m is a set of rules which leads to a hypothesis H_k , then H_k is satisfactory if all of R_1,... , R_m is satisfied. To analyze a rule, each of its components, e.g. CL_i, is validated. If all the components are true then the rule is valid.

2.1.5 Analysis of the passed hypotheses to choose the next state

Suppose the state *T* of *level-t* and the hypothesis *sublevel-d* in an iteration. Then two possibilities for the rule are:

A) The rule is not passed:

which indicates that all the hypotheses of sublevel-d are rejected. Therefore, the decision is transferred to the next sublevel (e.g. *d=d+1*). If *d* is equal to *t*, then the pixel belongs to one or more of the classes in *T*. Otherwise, the next iteration continues with *d* and the same state *T*.

B) The rule is passed:

Suppose the hypothesis was $T \longrightarrow D$. Then, the new state is $T = D$. If the level of this new state is one, the pixel is classified into a class in *new-S* and the analysis of the pixel is terminated. Otherwise, the new sublevel is *new-d=1*. The progress to the next iteration with *new-T* and *new-d* is continued.

2.2 Fuzzy Logic

There are three steps in a fuzzy method for the classification of remote sensing images. In the first step, the contribution of each class in each pixel is estimated using a fuzzification process with a proper membership function (MF). In this step, each pixel is converted to a matrix of membership degrees. In the second step, proper reasoning rules are applied to the fuzzy inputs (e.g. to the matrix of membership degrees) to achieve a fuzzy classification of pixels. In this step, normalization of data may be required. Lastly, in the third step, a defuzzification process is applied to create a hard classification output (Ghosh et al., 2014; Ghosh et al., 2010; Dutta, 2009; Xu et al., 2019; Al-Obeidat et al., 2015; Melgani et al., 2000; Zhao, 2008).

2.2.1 Fuzzification

The fuzzy domain includes several fuzzy sets representing the bands. Each fuzzy set (band) contains fuzzy subsets that indicate the land cover classes. Each fuzzy subset (e.g. land cover *c*), in a given fuzzy set (e.g. band *b*) is defined by a membership function, $f_{b,c}(x_b)$. where x_b is the value of the spectral pixel of $\underline{X}$ in the band *b* and land cover *c*.

In the proposed classifier, DTFL, seven different fuzzy membership functions were used for fuzzification including triangular shape, trapezoidal shape, π shape, bell shape, Gaussian, differential S shape and multiplicative S shape. The mathematical expression of each membership function is as the following (Momeni, 2011; Zhao, 2008; Matlab, 2017):

A) Triangular shape (Equ. 2)

$$Triangular(x,a,b,c) = \max\left\{\min\left\{\frac{x-a}{b-a}, \frac{c-x}{x-b}\right\}, 0\right\} \quad \text{(Equ.2)}$$

B) Trapezoidal shape (Equ. 3)

$$Trapezoidal(x,a,b,c,d) = \max\left\{\min\left\{\frac{x-a}{b-a}, 1, \frac{d-x}{d-c}\right\}, 0\right\} \quad \text{(Equ.3)}$$

C) π shape (Equ. 4)

$$Pi(x,a,b,c,d) = \begin{cases} 0 & x \le a \\ 2\left(\frac{x-b}{b-a}\right)^2 & a \le x \le \frac{a+b}{2} \\ 1-2\left(\frac{x-b}{b-a}\right)^2 & \frac{a+b}{2} \le x \le b \\ 1 & b \le x \le c \\ 1-2\left(\frac{x-c}{d-c}\right)^2 & c \le x \le \frac{c+d}{2} \\ 2\left(\frac{x-d}{d-c}\right)^2 & \frac{c+d}{2} \le x \le d \\ 0 & d \le x \end{cases} \quad \text{(Equ.4)}$$

D) Bell shape (Equ.5)

$$Bell(x,a,b,c) = \frac{1}{1+\left|\frac{x-c}{a}\right|^{2b}} \quad \text{(Equ. 5)}$$

E) Gaussian (Equ.6)

$$Gauss(x.m.s) = e^{\frac{-(x-m)^2}{2s^2}} \quad \text{(Equ.6)}$$

F) Differential S shape (Equ. 7)

$$Dsigm(x,a_1,c_1,a_2,c_2) = \frac{1}{1+e^{-a_1(x-c_1)}} - \frac{1}{1+e^{-a_2(x-c_{21})}} \quad \text{(Equ. 7)}$$

G) Multiplicative S shape (Equ. 8)

$$Psigm(x,a_1,c_1,a_2,c_2) = \frac{1}{1+e^{-a_1(x-c_1)}} \times \frac{1}{1+e^{-a_2(x-c_{21})}} \quad \text{(Equ.8)}$$

2.2.2 Reasoning rule

According to literature, a low fuzzy membership value MIN rule (so-called intersection rule) is a simple, fast and effective reasoning rule for many fuzzy problems (Ghosh et al., 2014; Ghosh et al., 2010; Melgani et al., 2000). In addition to the MIN rule, a high fuzzy membership value MAX rule (so-called union rule) is also considered as an effective reasoning rule (Ghosh et al., 2014; Ghosh et al., 2010; Melgani et al., 2000). However, intersection and union rules are generally not powerful enough for sophisticated classification processes where there are highly overlapped classes. In the current work, 12 different reasoning rules were used including minimum, maximum, multiplicative, collective, collective second power, mathematical mean, geometric mean, harmonic mean, minimum/ maximum, mathematical mean× minimum/ maximum, geometric mean × minimum/ maximum and harmonic mean ×minimum/ maximum. The mathematical expression of each reasoning rule is shown in the following (Momeni, 2011):

A) Minimum (Equ. 9): $f_c^{'}(x) = Min\{f_{1,c}(x),..., f_{B,c}(x)\}$ (Equ. 9)

B) Maximum (Equ. 10): $f_c^{'}(x) = Max\{f_{1,c}(x),..., f_{B,c}(x)\}$ (Equ. 10)

C) Multiplicative (Equ. 11): $f_c^{'}(x) = \prod_{b=1}^{B} f_{b,c}(x)$ (Equ. 11)

D) Collective (Equ. 12): $f_c^{'}(x) = \sum_{b=1}^{B} f_{b,c}(x)$ (Equ. 12)

E) Collective second power (Equ. 13): $f_c^{'}(x) = \sum_{b=1}^{B} f_{b,c}^2(x)$ (Equ. 13)

F) Mathematical mean (Equ. 14): $f_c^{'}(x) = \frac{1}{B}\sum_{b=1}^{B} f_{b,c}(x)$ (Equ. 14)

G) Geometric mean (Equ. 15): $f_c^{'}(x) = [\prod_{b=1}^{B} f_{b,c}(x)]^{1/B}$ (Equ. 15)

H) Harmonic mean (Equ. 16): (Equ. 16)

$$f_c^{'}(x) = \frac{B}{\sum_{b=1}^{B} \frac{1}{f_{b,c}(x)}}$$

I) Minimum / Maximum (Equ. 17):

$$f_c^{'}(x) = \frac{Min\{f_{1,c}(x),..., f_{B,c}(x)\}}{Max\{f_{1,c}(x),..., f_{B,c}(x)\}} \quad \text{(Equ. 17)}$$

J) Mathematical mean × Minimum / Maximum (Equ. 18):

$$f_c^{'}(x) = \frac{1}{B}\sum_{b=1}^{B} f_{b,c}(x) \times \frac{Min\{f_{1,c}(x),..., f_{B,c}(x)\}}{Max\{f_{1,c}(x),..., f_{B,c}(x)\}} \quad \text{(Equ. 18)}$$

K) Geometric mean × Minimum / Maximum (Equ. 19):

$$f_c^{'}(x) = [\prod_{b=1}^{B} f_{b,c}(x)]^{1/B} \times \frac{Min\{f_{1,c}(x),..., f_{B,c}(x)\}}{Max\{f_{1,c}(x),..., f_{B,c}(x)\}} \quad \text{(Equ. 19)}$$

L) And Harmonic mean × Minimum / Maximum (Equ. 20):

$$f_c^{'}(x) = \frac{B}{\sum_{b=1}^{B} \frac{1}{f_{b,c}(x)}} \times \frac{Min\{f_{1,c}(x),..., f_{B,c}(x)\}}{Max\{f_{1,c}(x),..., f_{B,c}(x)\}} \quad \text{(Equ. 20)}$$

2.2.3 Defuzzification

In the proposed classifier, DTFL, the last step is a hard classification using MAX or MIN operations as the simplest defuzzifiers. Other defuzzification methods, such as centroid of the area or mean of maximum, are used in other problems such as control systems (Momeni, 2011; Ghosh et al., 2014; Ghosh et al., 2010). However, in the proposed approach, DTFL, each pixel is assigned to the class *c* with the highest membership value using the MAX operator. The mathematical expression of the MAX operator is as:

MAX: $\forall j \in 1,2,\ldots,c \quad and \quad j \neq c, F_c(x) \geq F_j(x)$ (Equ. 21)

where $F_j(x)$ is the membership value for the j[th] class (Momeni, 2011).

Figure 3 illustrates the flowchart of classification using DTFL. In that flowchart, two parts of DTFL, the decision tree and the fuzzy logic, are shown simultaneously.

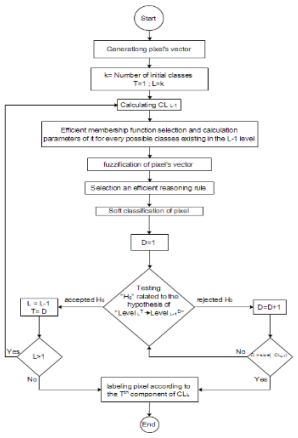

Figure 3: Flowchart of DTFL classifier

3. Experimental Results

In order to evaluate the accuracy and performance of the proposed method, a GeoEye-1 satellite image of Azadi Stadium, Iran, (Figure 4) was classified using DTFL. In the study area nine different dominant classes were determined as "blue-seats" and "white-seats" from the first floor of the stadium, "lawn" and "soil" and "pedestrian-gravel" from the playing fields, "concrete-seats" from second floor of the stadium, "asphalt-road" and "cement-wall" from the surrounding of the stadium, and "water" from northern lake of the stadium. The GeoEye-1 image was taken on Jan 07, 2009 with GSD of 16 inches (0.41 m) in panchromatic mode and GSD of 65 inches (1.65 m) in a multispectral mode with 11 bits per pixel as radiometric resolution (Momeni et al., 2018; Bagheri et al., 2011). Even though GeoEye-1 is able to acquire images with a resolution of 41 cm, but under the company's current operating license from the National Oceanographic and Atmospheric Agency (NOAA) images must be resampled down to half a meter for commercial customers (Momeni et al., 2018). This resampling will mix up some pixels and classes and decreases the accuracy of classification.

A set of training data were used to estimate the statistical parameters of each class for each reasoning rule. In this study, training data were collected based on 1:2000 topographic maps and ground surveying. Finally, the satellite image of the study area was classified using DTFL with seven different fuzzy membership functions and 12 different decision rules. Membership functions included triangular shape, trapezoidal shape, π shape, bell shape, Gaussian, differential S shape and multiplicative S shape. Decision rules included Minimum, Maximum, Multiplicative, Collective, Collective second power, mathematical mean, geometric mean, harmonic mean, minimum/ maximum, mathematical mean × minimum/ maximum, geometric mean × minimum/ maximum and harmonic mean × minimum/ maximum.

Table 1 and Table 2 summarize the Kappa coefficients and overall accuracies of image classification using DTFL.

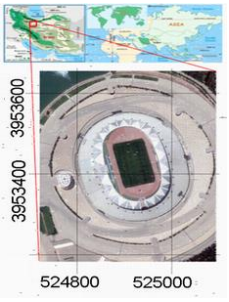

Figure 4: GeoEye-1 satellite image of Azadi Stadium (Tehran, Iran)

Table 1: Kappa coefficients of classification using DTFL with different membership functions

	Membership function						
	Triangular shape	Trapezoidal shape	π shape	Bell shape	Gaussian	Differential S shape	Multiplicative S shape
Minimum	96.07	94.66	95.55	94.17	95.61	95.55	95.55
Collective	95.57	93.74	94.82	93.85	94.93	94.82	94.82
Multiplicative	94.65	92.24	93.61	91.65	93.94	93.61	93.61
Maximum	95.25	94.03	94.90	94.23	94.75	94.90	94.90
Minimum /Maximum	95.95	94.06	93.25	63.23	95.36	93.25	93.25
Collective second power	95.31	93.53	94.65	93.65	94.70	94.65	94.65
Mathematical mean	95.00	93.08	94.32	93.33	94.30	94.32	94.32
Geometric mean	95.82	94.38	95.59	95.13	95.33	95.59	95.59
Harmonic mean	**96.09**	94.76	95.87	95.25	95.62	95.87	95.87
Mathematical mean × Minimum / Maximum	95.54	93.53	94.56	92.72	95.08	94.56	94.56
Geometric mean × Minimum / Maximum	95.42	92.85	94.14	91.77	94.75	94.14	94.14
Harmonic mean × Minimum / Maximum	95.26	92.39	93.59	90.99	94.41	93.59	93.59

Table 2: Overall accuracies of classification using DTFL with different membership functions

	Membership function						
	Triangular shape	Trapezoidal shape	π shape	Bell shape	Gaussian	Differential S shape	Multiplicative S shape
Minimum	96.12	94.73	92.33	94.25	95.67	95.60	95.60
Collective	95.63	93.83	92.18	93.93	94.99	94.89	94.89
Multiplicative	94.72	92.34	90.05	91.76	94.02	93.69	93.69
Maximum	95.32	94.11	92.76	94.30	94.82	94.97	94.97
Minimum /Maximum	96.00	94.14	91.69	63.70	95.42	93.34	93.34
Collective second power	95.38	93.61	92.11	93.74	94.77	94.72	94.72
Mathematical mean	95.07	93.17	91.68	93.42	94.37	94.39	94.39
Geometric mean	95.87	94.46	92.87	95.19	95.39	95.65	95.65

Harmonic mean	**96.14**	94.83	92.92	95.31	95.68	95.93	95.93
Mathematical mean × Minimum / Maximum	95.60	93.61	90.91	92.81	95.15	94.63	94.63
Geometric mean × Minimum / Maximum	95.48	92.95	90.08	91.87	94.82	94.22	94.22
Harmonic mean × Minimum / Maximum	95.32	92.49	88.39	91.10	94.48	93.67	93.67

4. Discussion

To prove the performance of image classification using DTFL, the results were compared with the results of the Maximum Likelihood classification. The best result of DTFL (using triangulation shape membership function and harmonic mean as reasoning rule) is compared with the result of the Maximum Likelihood (ML) in Table 3.

Table 3: Summary of the image classification by ML and DFTL

Classifier	Overall accuracy (%)	Kappa coefficient (%)
ML	89.91	89.77
DTFL	96.14	96.06

From Table 1 to Table 3, it is concluded that the results of classification by DTFL in the best mode (using a triangular-shaped membership function and harmonic-mean as reasoning rule) is better than the results of ML classifier. DTFL improves the accuracy of the classification for more than 6% in comparison with ML. In practice, it is common to use a threshold in the ML classifier to increase the accuracy and precision of the classification (Momeni, 2011). In this case, low-reliability pixels are excluded from the classification process and get a non-classified label. Therefore, the accuracy of the rest of the pixels in the classification will be improved. By defining a threshold in the ML method to achieve the same accuracy of the DTFL in this case study, 8.73% of the pixels took the non-classified label. Therefore, using ML 8.73% of pixels are excluded in the future decision makings as there is no idea about their mixed contents. However, as it already mentioned in Section Two, DTFL is able to classify all the pixels and avoids non-classification labels. Therefore, using DTFL, we have more knowledge about mixed pixels and their contents. The confusion matrix resulted from DTFL (using triangulation shape membership function and harmonic mean as reasoning rule) is shown in Table 4.

Table 4: Confusion matrix resulted by DTFL classifier

True Class / Resulted class	C_1	C_2	C_3	C_4	C_5	C_6	C_7	C_7	C_9	Sum
Mixed of C_1&C_2&C_4&C_5&C_7&C_8&C_9	0	0	0	0	0	1	0	0	0	1
Mixed of C_2&C_4&C_6&C_8	0	0	0	13	0	0	0	0	0	13
Mixed of C_2&C_4&C_6	0	0	0	1	0	0	0	0	0	1
Mixed of C_2&C_3&C_9	0	0	3	0	0	0	0	0	0	3
Mixed of C_2&C_3	0	0	2	0	0	0	0	0	0	2
Mixed of C_2&C_5	0	5	0	0	18	0	0	0	0	23
Mixed of C_1&C_7	0	0	0	0	0	0	4	0	0	4
Mixed of C_4&C_7	0	0	0	0	0	0	5	0	0	5
Mixed of C_1&C_8	0	0	0	2	0	0	0	0	0	2
Mixed of C_2&C_8	0	0	0	0	0	0	0	5	0	5
Mixed of C&C_8	0	0	0	1	0	0	0	0	0	1
Mixed of C_3&C_9	0	0	37	0	0	0	0	0	35	72
C_1	178	0	0	1	0	0	3	0	0	182
C_2	2	287	0	0	40	0	0	10	0	339
C_3	0	0	4982	0	0	0	0	0	189	5171
C_4	0	0	0	555	0	0	1	0	0	556
C_5	1	6	0	0	266	0	0	0	0	273
C_6	0	0	0	0	0	485	0	0	0	485
C_7	0	0	0	0	0	0	289	0	0	289
C_8	0	0	0	3	0	0	0	315	0	318
C_9	0	0	138	0	0	0	0	0	5741	5879
Sum	181	298	5162	576	324	486	302	330	5965	13624 / 13624
No. Ground-Truth pixels	181	298	5162	576	324	486	302	330	5965	13624
No. Non-classified pixels	0	0	0	0	0	0	0	0	0	0

Where C_1 to C_9 are "blue-seats", "white-seats", "lawn", "soil", "pedestrian-gravel", "concrete-seats", "asphalt-road", "cement-wall" and "Water", respectively. Also, the confusion matrix resulted from an ML classifier is shown in Table 5.

Table 5: Confusion matrix resulted in ML classifier

True Class / Resulted class	C_1	C_2	C_3	C_4	C_5	C_6	C_7	C_7	C_9	Sum
C_1	158	0	0	0	0	0	1	4	0	163
C_2	0	231	0	0	2	0	0	0	0	233
C_3	0	0	4454	0	0	0	0	0	267	4721
C_4	0	0	0	556	0	0	0	0	0	556
C_5	3	59	0	0	322	0	0	2	0	386
C_6	0	0	0	0	0	486	0	0	0	486
C_7	3	0	0	3	0	0	298	0	0	304
C_8	3	1	0	9	0	0	0	309	0	322

C_9	0	0	191	0	0	0	0	0	5073	5264
Sum	167	291	4645	568	324	486	299	315	5340	12435 / 12435
No. Ground-Truth pixels	181	298	5162	576	324	486	302	330	5965	13624
No. Non-classified pixels	14	7	517	8	0	0	3	15	625	1189 ≈8.73%

Where C_1 to C_9 are "blue-seats", "white-seats", "lawn", "soil", "pedestrian-gravel", "concrete-seats", "asphalt-road", "cement-wall" and "Water", respectively.

As Table 4 and Table 5 show, due to the threshold in ML to obtain the same accuracy as DTFL, 1189 pixels have been excluded from the classification process and there is no idea about their contents. However, using DTFL only 117 pixels were detected as mixed pixels while we know the contribution of possible classes in those pixels. Thus, we will have valuable information about the contribution of each class in those pixels. That information helps regional planners and agricultural managers to more realistic future planning.

5. Conclusion

In this paper, we proposed a novel classifier, DTFL, based on fuzzy logic and decision tree. At the beginning of classification, each pixel is located at the highest level of a decision tree. At that level, each pixel belongs to the combination of all initial classes. DTFL classifies each pixel in a fewer number of classes using some hypotheses. As DTFL transfers a pixel from higher levels of the tree to the lower levels, the uncertainty about the contents of the pixel decreases. Decision making about transfers and hypotheses are based on fuzzy logic. In the classification of a GeoEye-1 satellite image, DTFL reached the overall accuracy of 96.14% and the Kappa coefficient of 96.06% using triangular membership function and harmonic mean reasoning rule. DTFL reached a higher accuracy in comparison with the overall accuracy of 89.91% and the kappa coefficient of 89.77% resulted in a Maximum Likelihood classification. Defining a threshold in the Maximum Likelihood method to obtain the same accuracy as the DTFL leaves 8.73% of pixels without any label (as non-classified pixels). However, DTFL was able to assign a proper label to all pixels.

The results of this study approved the performance of the proposed classifier, DTFL. However, in order to improve the classifier, including other types of membership functions, such as L-function, in the fuzzy logic is suggested. In addition, applying DTFL to study less-distinctive agricultural products using multi-spectral satellite images may better reveal the strength of DTFL. Including advanced artificial intelligence methods, such as a genetic algorithm, to the training section of the proposed method may improve the overall accuracy as well as the Kappa coefficient of the classification. Also, as future studies, researchers may modify and improve DTFL for unsupervised classification of satellite images.

References

Akgun, A., Eronat, A., Turk, N., 2004. Comparing different satellite image classification methods: an application in ayvalik district, western Turkey. XXth ISPRS Congress, Retrieved from http://citeseerx.ist.psu.edu/viewdoc/download?doi=10.1.1.643.3422&rep=rep1&type=pdf

Al-Obeidat, F., Al-Taani, A., Belacel, N., 2015. A fuzzy decision tree for processing satellite images and Landsat data. Procedia Computer Science. Procedia Computer Science, 52, 1192-1197. doi: https://doi.org/10.1016/j.procs.2015.05.157

Bagheri, S.M.P., Momeni, E., Fard, F.S.N., 2011. Updating urban maps using GeoEye stereo pair satellite images. Shahrnegar, 55(12), 103-112.

Bai, Y., Feng, M., Jiang, H., 2014. Assessing the consistency of five global land cover data sets in China. Remote Sensing, 6(9), 8739-8759. DOI:10.3390/rs6098739

Dutta, A., 2009. Fuzzy c-mean classification of multispectral data incorporating spatial contextual information by using Markov random field (Master thesis). International Institute for Geo information Science and Earth Observation. Retrieved from:

Ghosh, A., Shankar, U., Bruzzone, L., 2010. Neuro-fuzzy-combiner: effective multiple classifier systems. International Journal of Knowledge Engineering and Soft Data Paradigms, 2(2), 107-129. DOI: 10.1504/IJKESDP.2010.034678

Ghosh, S., Biswas, S., Sarkar, D., 2014. A novel neuro-fuzzy classification technique for data mining. Egyptian Informatics Journal, 15, 129–147, https://doi.org/10.1016/j.eij.2014.08.001

Gómez, C., White, J., Wulder, M., 2016. Optical remotely sensed time series data for land cover classification: A review. ISPRS Journal of Photogrammetry and Remote Sensing, 55–72. https://doi.org/10.1016/j.isprsjprs.2016.03.008

González, M., Minuesa, C., del Puerto, I., 20161. Maximum likelihood estimation and expectation–maximization algorithm for controlled branching processes. Computational Statistics and Data Analysis, 93, 209–227. https://doi.org/10.1016/j.csda.2015.01.015goo.gl/nLkxkh

Joseph, G., Chockalingam, J., 2017. Fundamentals of Remote Sensing. Universities Press, ISBN: 9789386235466.

Matlab. 2017. Fuzzy logic toolbox, MatLab

Melgani, F., Hashemy, B., Taha, S., 2000. An explicit fuzzy supervised classification method for multispectral remote sensing images. IEEE transactions on geoscience and remote sensing, 38(1), 287-295. DOI: 10.1109/36.823921

Momeni, E., 2011. Satellite image classification by tree method and fuzzy algorithm (Master's thesis). Retrieved from: https://ganj.irandoc.ac.ir/articles/524840

Momeni, E., Fard, F.S.N., Haghi, H., 2018. Accuracy Assessment of GeoEye-1 Satellite Images for Updating Large-Scale Maps in Iran. Journal of Geography & Natural Disasters, 8 (1). DOI: 10.4172/2167-0587.1000219

Weng, Q., Lu, D., 2007. A survey of image classification methods and techniques for improving classification performance. International Journal of Remote Sensing, 28(5), 823–870. DOI: 10.1080/01431160600746456

Xu, J., Feng, G., Zhao, T., Sun, X., Zhu, M., 2019. Remote sensing image classification based on semi-supervised adaptive interval type-2 fuzzy c-means algorithm. Computers & Geosciences, 131, Pp. 132-143. https://doi.org/10.1016/j.cageo.2019.06.005

Zhao, X., 2008. A. Stein, Integration of multi-source information via a fuzzy classification method for wetland grass mapping. The International Archives of the Photogrammetry, Remote Sensing, and Spatial Information Sciences, XXXVII(Part B7), 1463-1470, Retrieved from https://www.isprs.org/proceedings/XXXVII/congress/7_pdf/9_ThS-17/11.pdf

Zimmermann, H., 2011. Fuzzy set theory and its applications. Springer. Retrieved from https://pdfs.semanticscholar.org/a31d/fa5eb97fced9494dfa1d88578da6827bf78d.pdf.